

## 10A.4 Hail detection and quantification with a C-band polarimetric radar :

### Challenges and promises

P. Tabary<sup>1</sup>, B. Fradon<sup>1</sup>, P. Dupuy<sup>1</sup>, A.J. Illingworth<sup>2</sup> and G. Vulpiani<sup>3</sup>

<sup>1</sup> Centre de Météorologie Radar, Direction des Systèmes d'Observation, Météo France, Toulouse, France

<sup>2</sup> U. Reading, Reading, UK

<sup>3</sup> Dept. of Civil Protection, Rome, Italy

phase  $K_{DP}$ ) allows improving the distinction between heavy rain, dry hail and wet, melting hail.

#### 1. Introduction

Among the various meteorological risks, hail is certainly one of the least understood, measured and forecasted. This is in part due to the extremely high space-time variability of the phenomenon as well as to the complexity of the microphysical and kinematical processes that are involved. In contrast with that, the economic consequences of hail storms can be devastating in sectors like agriculture, aviation, car manufacturing, ... A well known example is the 1984 Munich hailstorm that caused about 1.5 B€ damages, about half of which were insured (SwissRe, 2006). More recently a hail storm hit the city of Toulouse (SW of France) on the 25<sup>th</sup> of May, 2009, impacting about 70,000 cars. The average repair amount per car is estimated to be 3,000 euros.

Radars, because of their ability to monitor the 3D structure of storms at very high space-time resolutions (5 minutes and 1 km<sup>2</sup>), have been long recognized as the main tool to detect and quantify hail. Early approaches relied either on reflectivity thresholds (55 dBZ or so, Donaldson 1959) applied to PPIs or pseudo-CAPPI, or on 3D-derived information such as echo tops, Vertically Integrated Liquid Water (VIL, Amburn and Wolf 1997) or the height difference between the 45 dBZ isopleth and the freezing level. The latter, often referred to as the Probability Of Hail (POH, Waldvogel et al. 1979, Delobbe and Holleman 2006), is supposed to be the best candidate among all conventional algorithms. Most operational radar services have introduced conventional algorithms for hail detection.

The advent of polarimetry into operational networks opens new perspectives. First off, polarimetry allows better distinguishing meteorological from non-meteorological targets (e.g. ground-clutter). Secondly, polarimetry (and specifically the differential phase  $\phi_{DP}$ ) offers a means to correct if not all a significant fraction of the precipitation-induced attenuation, which is quite frequent in hail-bearing convective systems. Finally, the availability of additional parameters (differential reflectivity  $Z_{DR}$ , correlation coefficient  $\rho_{HV}$  and specific differential

#### 2. The French polarimetric radars and the hailpad network used for validation

The French operation radar network will comprise 10 polarimetric systems at the end of 2009 (9 are C-band and 1 is S-band, see Fig. 1 below). All systems were manufactured by SELEX and operate in STAR (Simultaneous-Transmit-And-Receive Mode) mode. The transmitter and the receivers are both in the shelter below the antenna. A dual-rotary joint connects the moving and stationary wave guides.

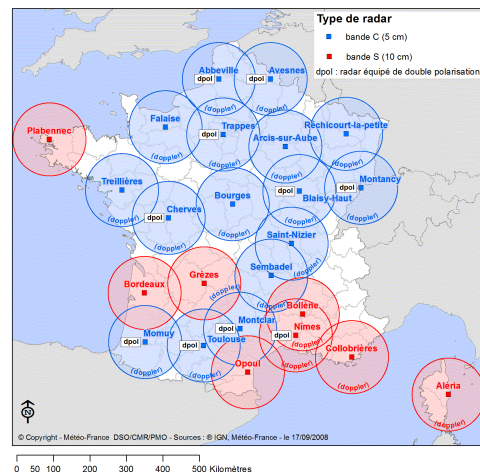


**Figure 1 : map of the French radar network at the end of 2009. Red (blue) coverage domains correspond to S-band (C-band) radars. The “dpol” labels indicate the dual-polarization systems at the end of 2009.**

The quality of the first installed polarimetric radar (Trappes, near Paris) has been thoroughly assessed (Gourley et al. 2006). Significant work has been carried out since then to 1) separate precipitation from non-precipitation echoes (Gourley et al. 2007), 2) document - and propose solutions to - attenuation at C-band (Gourley et al. 2006b, Vulpiani et al. 2008, Tabary et al. 2009), 3) improve the calibration of reflectivity and differential reflectivity (e.g. Gourley et al. 2009). The present study was conducted using the C-band Toulouse radar (located in the SW of France, see Fig. 1). The reason for that is the SW of France is

a region that is prone to hail events. The following Figure (Fig. 2) is a damage-based climatology of hail falls over France :

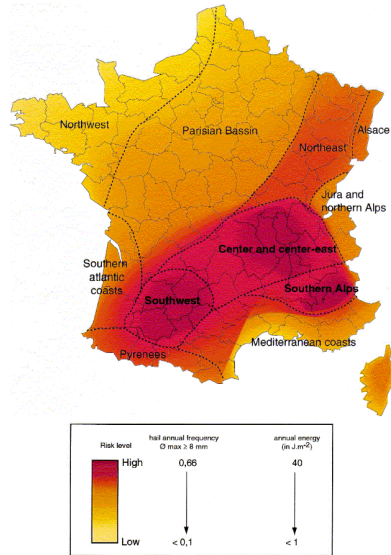


**Figure 2 : Spatial distribution of hail risk in France (taken from Vinet 2001).**

The SW of France is also a region where vineyards are grown and expensive wines (e.g. Bordeaux) are produced. The economic stakes regarding hail detection, climatology and forecasting are thus very high. This, combined with the high occurrence of severe hail lead a farmer's association, called ANELFA (Association Nationale d'Etude et de Lutte contre les Fléaux Atmosphériques, Dessens 1986), to deploy over the years a dense network of hailpads (see Fig. 3 below). Each hailpad, the surface of which is  $1 \text{ m}^2$ , is checked after every precipitation event, whatever its severity was. If the hailpad is found not to be impacted, then it is kept in place. Otherwise, the pad is inked, analyzed and replaced by a new one. The pad analysis is stored into the ANELFA database. It consists in the event-cumulated surface Hailstone Size Distribution (the first diameter in the distribution being  $5 \text{ mm}$ ) as well as integrated parameters such as the hail kinetic energy, mass, ... The hailpad data do not contain the exact timing or duration of the hailfall within the day. Assumptions have to be made (event durations, hailstone terminal fall speeds, ...) to retrieve the volumetric Hailstone Size Distribution, which is needed for polarimetric radar simulations. We made the assumption that if no hail report was available in the ANELFA database for a given hailpad, it means that no hail occurred at the considered hailpad's location. The ANELFA managers confirmed it was a fair assumption and that, over one season, only a very small percentage of all hailpads could not be checked (due for instance to farmers's unavailability) after all precipitation events. The conclusion of that is that a hailpad that is missing in the database can be interpreted as an observation of NO-HAIL. We remind here that, given the

characteristics of the hailpads, NO-HAIL means that the hailstones, if any, all had a diameter less than  $5 \text{ mm}$ .

The advantage of having NO-HAIL observations is that the False Alarm Rate (FAR) can be computed rigorously in our study. This score, unlike the Probability Of Detection (POD), is always a difficult one to compute for rare, localized, short-duration and high-impact weather phenomena (windshears, tornadoes, hail, ...).

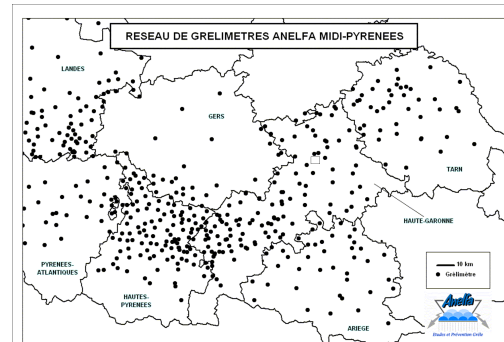


**Figure 3 : The ANELFA hailpad network around the Toulouse radar. The black lines are the limits of the French administrative entities (Départements). Each hailpad is plotted as a black dot. There are several hundreds of them within the 80 range circle of the Toulouse radar (square).**

### 3. Radar data processing : a qualitative illustration of the challenges posed by hail detection at C-band

As mentioned above, the radar data processing is achieved by a modular chain that handles sequentially the various error sources.

First off, reflectivity ( $Z_H$ ) and differential reflectivity ( $Z_{DR}$ ) are corrected for azimuth-dependent biases. That step is extremely important for hydrological products, for which the required accuracies on  $Z_H$  and  $Z_{DR}$  are about 1 and 0.2 dB. For hydrometeor classification, however, an accuracy of 2 and 0.4 dB on  $Z_H$  and  $Z_{DR}$  is acceptable.

The second step consists in separating precipitation from non-precipitation echoes. We apply here the Gourley et al. (2007) fuzzy logic methodology, which is based on  $Z_H$ ,  $\rho_{HV}$ ,  $\sigma_Z$  (pulse-to-pulse reflectivity fluctuation), texture of  $Z_{DR}$  with empirically determined membership functions (MF). The MF had however to be adapted because they were initially tuned for the Trappes (Paris) area, which is rather flat. The Toulouse radar is located in a more rugged environment, with a large and high (3,000 m) mountain range (Pyrénées) between 60 and 120 km in the south of the radar. *Unexpectedly with respect to our previous Trappes ("flat terrain") experience, high  $\rho_{HV}$  (up to 0.99) were found in that sector, resulting initially in misclassified clutter pixels at high reflectivity levels (60 dBZ or so), which were subsequently*

classified as hail in the final hydrometeor classification module. The  $\rho_{HV}$  membership function was modified accordingly.

The next step consists in determining and removing the  $\phi_{DP}$  (azimuth-dependent) offset. We call that step the “ $\phi_{DP}$  normalization” step. Then, the normalized  $\phi_{DP}$  profile is filtered and  $K_{DP}$  is estimated. The  $\phi_{DP}$  normalization can be done either dynamically, using a  $\phi_{DP0}$  estimation for each ray, with some sort of azimuthal continuity being imposed. The advantage is that any change in the  $\phi_{DP0}$  offset is automatically accounted for. The drawback is that if the first gates are not classified as precipitation (e.g. because of the presence of strong ground-clutter) and there is rain causing attenuation at very close range around the radar, then the dynamic  $\phi_{DP0}$  will not catch the attenuation that occurred between the radar and the first precipitation-classified gates. The other approach consists in using a static  $\phi_{DP0}=f(\text{azimuth})$  curve, which is updated on a daily basis. In the present work, we used the static normalization. The  $\phi_{DP}$  profile is then filtered by applying a running 25-gates median filter. As the gate width is 240 m, this corresponds to a filtering length of 6 km. This may seem high but several tests have been conducted and this conservative, robust filtering length was preferred. At least 13 out of 25 gates have to be precipitation-classified to validate the estimated filtered  $\phi_{DP}$ .  $K_{DP}$  is finally estimated by performing a linear regression over 25 filtered  $\phi_{DP}$  gates. *It should be kept in mind – particularly if simulation, T-matrix-based results are to be used - that this  $K_{DP}$  estimation, because of the way  $\phi_{DP}$  is filtered, is very likely to underestimate the intrinsic  $K_{DP}$  in convective cells.*

The next step is the attenuation correction, which is done assuming a linear relationship between  $A_H$  and  $A_{DP}$  (specific attenuation and specific differential attenuation) and  $K_{DP}$  (specific differential phase). The coefficients of proportionality,  $\gamma_H$  and  $\gamma_{DP}$ , were assumed to be constant and respectively equal to 0.08 and 0.03 dB km<sup>-1</sup>. This is a simplification over what can be observed in reality. Indeed, Tabary et al. (2009), using a physical approach and two years of Trappes radar data in convection, have shown that  $\gamma_{DP}$  can vary in the range [0.01 – 0.1] dB km<sup>-1</sup> pending upon the microphysics of attenuating cells. Figure 4, taken from Tabary et al. (2009), is a good illustration of that variability. It shows the Path Integrated Differential Attenuation (PIDA) as a function of  $\phi_{DP}$  for different values of the (intrinsic)  $Z_{DR}$  values of convective cells.  $\gamma_{DP}$  is the slope of the curves.

The highest  $\gamma_{DP}$  values, were associated to the so-called “hot spots”, i.e. convective cells containing either extremely large drops or melting hailstones (both of them leading potentially to resonance effects) and causing unusually high differential attenuation. *Hot spots have been found to be quite frequent in intense, hail-bearing storms and one has to admit that it is quite complicated to correct for the induced*

attenuation. The corrected  $Z_{DR}$  may thus be either overestimated or underestimated, which in turn may lead to 1) either heavy rain being classified as hail (False Alarm) or 2) hail being classified as heavy rain (Non Detection). *As an example, attenuation-corrected  $Z_{DR}$  that remain negative is always suspicious and can either be interpreted as rain with insufficient attenuation correction or, assuming the attenuation correction was correct, as hailstones falling with their major axis along the vertical.*

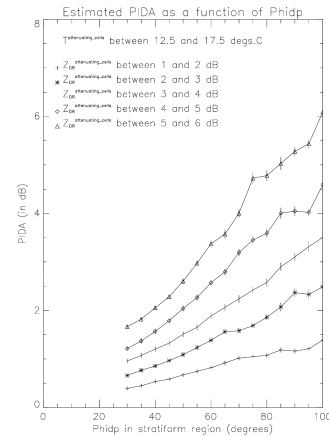


**Figure 4 : Illustration of the  $\gamma_{DP}$  (to be interpreted as the slope of the curves) variability as a function of the  $Z_{DR}$  of attenuating cells (from Tabary et al. (2009)).**

Cases of complete extinction have also been noted in several instances with the Toulouse (C-band) radar.

The last challenge in hail identification is related to our knowledge, or lack of knowledge, of the hail microphysics in convective precipitation and its impact of polarimetric variables. Several studies have reported on the many different habits and fall modes that hail can take in convective precipitation :

- dry, spherical or not spherical but tumbling hailstones;
- melting hailstones with a solid ice core covered by a torus of water (Rasmussen and Heymsfield 1987);
- large, dry, oblate hailstones falling with their major axis along the vertical (Zrnic et al. 1993);

This clearly makes the determination of the membership functions quite complicated. Indeed,  $Z_{DR}$  values, for instance, can vary from very negative (case of vertically aligned hailstones) to very positive (case of melting hailstones). Large, dry hailstones or hailstones mixed with rain will produce low  $\rho_{HV}$  (0.8 – 0.9) and  $\rho_{HV}$  is a parameter that has often been advertised to discriminate rain from hail. However, at

C-band resonance effects in heavy rain are quite common, leading also to low  $\rho_{HV}$  values.

Figure 5 and 6 present two radials (from top to bottom  $Z_H$ ,  $Z_{DR}$ ,  $K_{DP}$ ,  $\rho_{HV}$  and Hydrometeor Type) across two hail-bearing cells (confirmed by ground observations). In both cases,  $Z_H$  is extremely high (the maximum, identified by a vertical line is above 60 dBZ), (filtered)  $K_{DP}$  is moderate ( $2^\circ \text{ km}^{-1}$ ),  $\rho_{HV}$  is low (0.9) or extremely low (0.8). It should be noted that  $\rho_{HV}$  remains low at farther ranges even in low-to-moderate precipitation (probably because of reflectivity gradients). The  $Z_{DR}$  in the two examples, however, is extremely different. In one case (24<sup>th</sup> of May 2008), it reaches values as low as  $-5$  dB whereas in the other case (15<sup>th</sup> of May 2008) it goes up to  $+6$  dB.

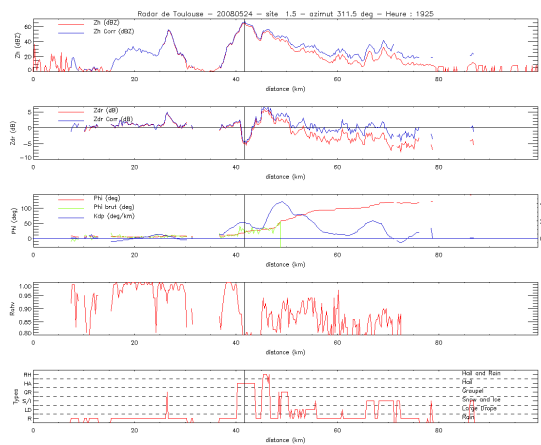


**Figure 5 : One particular ray at  $1.5^\circ$  elevation through a hail-bearing cell (confirmed by ground observations). Date / Time is 24<sup>th</sup> of May, 2008, 19.25 UTC.**

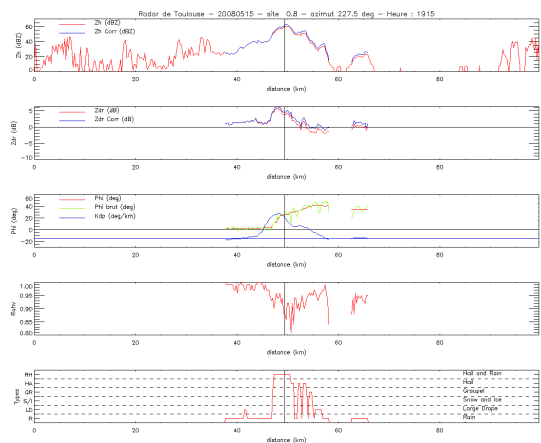


**Figure 6 : One particular ray at  $0.8^\circ$  elevation through a hail-bearing cell (confirmed by ground observations). Date / Time is 15<sup>th</sup> of May, 2008, 19.15 UTC.**

Figs. 7, 8 and 9 give the  $\rho_{HV}$ ,  $Z_{DR}$  and  $K_{DP}$  membership functions used for heavy rain, hail and

rain / hail (to be interpreted as Melting Hail). Temperature is also taken into account in the fuzzy logic scheme (adapted from Marzano et al. (2007)).

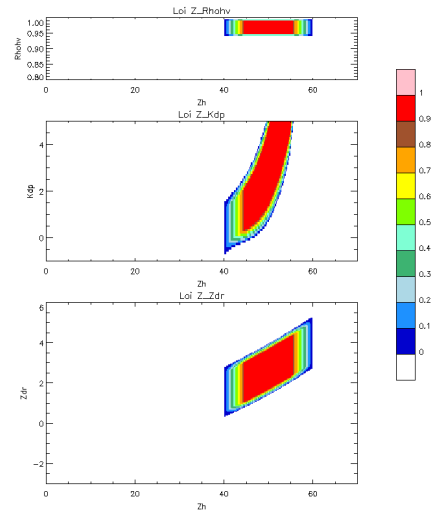


**Figure 7 : Heavy rain membership functions.**

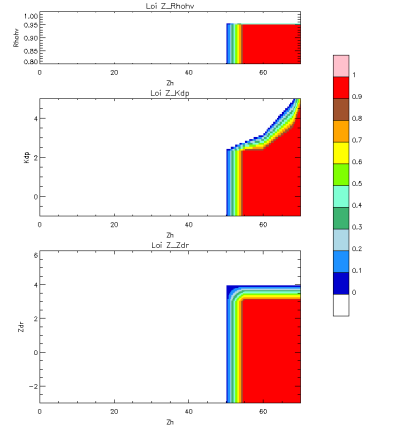


**Figure 8 : Hail membership functions.**

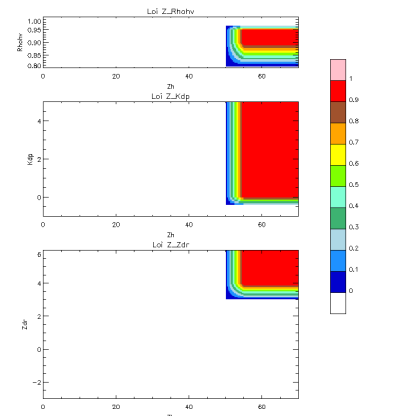


**Figure 9 : Rain / Hail (melting Hail) membership functions.**

The weights applied to  $\rho_{HV}$ ,  $Z_{DR}$  and  $K_{DP}$  are static and respectively equal to 2, 1 and 0.5. No dependency on Signal-to-Noise Ratio, differential phase, reflectivity gradients, ... (Park et al. 2009) has been tested yet.

#### 4. Quantitative results

The performance of the hail identification algorithm using the membership functions described above was assessed over the period May - September 2008, which covers 6 hail episodes where both radar data and hailpad observations are available (45 hail observations over a total of 1634 'hail' and 'nohail' observations).

Figure 10 shows the hail imprints over the different hours (in different colours) on the 15 May 2008. The white circle corresponds to a radar range of 50 km. Data at 0.8° elevation angle (revisited every 5') were used to produce that map. Permanent ground clutter areas are represented in grey. Only the class 'Hail' of the fuzzy logic algorithm was considered. Crosses indicate the hailpad locations, in red when hail (again with diameter > 5 mm) was detected, in white otherwise. There is an overall fair agreement between the radar diagnostics and the hailpad reports. Noteworthy is the extremely high variability of hail impacts, with impacted and not impacted hailpads coexisting within less than 2 – 3 km. Considering the density of white crosses (i.e. not impacted hailpads), there are an evident area of False Alarms in the SW sector of the radar between 10 and 40 km.

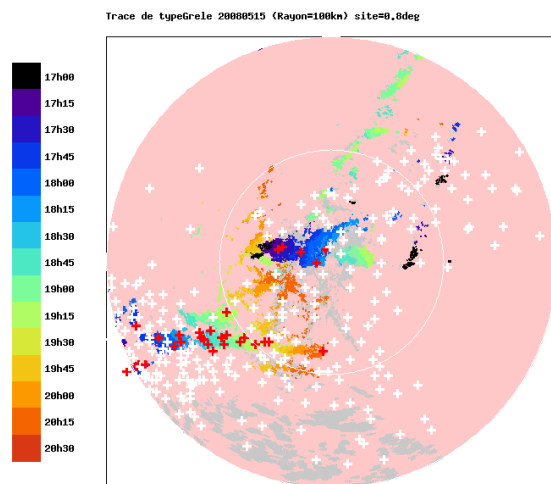


**Figure 10 : Hail imprints on the 15 May 2008. The crosses are the hailpads, in red when hail was observed**

The POD and FAR were calculated using 3 different algorithms for identifying hail :

- a simple threshold (55 dBz) on the 1.5° attenuation corrected horizontal reflectivity PPIs ( $Z_H$ ). Results are respectively 82 and 72%,

- the "Hail" type of the polarimetric fuzzy logic scheme applied to 1.5° PPIs. Results are respectively 84 and 76%,
- the Probability Of Hail (POH) computed from the 15' – 2.5 km nation-wide 3D reflectivity fields (Dupuy et al. 2009, this conference). The formula that is used is (Delobbe and Holleman 2006):  $POH = 0.319 + 0.133 * (H_{45dBZ} - H_{0Cisotherm})$ . Results are respectively 82 and 64%.

The radar-based hail diagnostics have been enlarged by 1 km in all 4 directions before comparison with the hailpad. The objective was to mitigate stroboscopic effects due to 5' revisit time. That might explain the rather high FAR obtained with all approaches. A better approach would consist in using the advection field to interpolate between successive hail detection maps. The POD is quite similar for the 3 methods, though slightly better with the polarimetric approach. The missed detections can be explained by an under-correction of the attenuation, extinction of the radar signal or by inappropriate membership functions.

#### 5. Conclusions and outlook

Based on this initial study, it appears that hail detection and quantification with a C-band dual-polarization radar is not straightforward. More work is needed and more cases should to be considered before arriving at final conclusions. The lessons that we can draw from this first experience are the following :

□ Efficient ground-clutter removal is very important. With no surprise, any deficiency in that preliminary step results in increased False Alarm Rates (FAR). Algorithms distinguishing between precipitation and non precipitation echoes have to be adapted according to the radar environment (mountainous vs. flat terrain) ;

□ Attenuation is systematic at C-band in hail-producing convective situation and should therefore be corrected for. The attenuation caused by the so-called "hot spots", i.e. cells containing very large drops and / or melting hailstones, can be dramatic, leading to complete extinction of the radar signal (even at C-band and at close ranges).

□ Resonance effects at C-band make the distinction between heavy rain with large drops and hail complicated. In particular,  $\rho_{HV}$ , the correlation coefficient, can not be considered as THE discriminating parameter. Low  $\rho_{HV}$  values (0.9 or even 0.8) have been observed in hail-bearing cells, in heavy rain and also in moderate high-SNR precipitation downstream of attenuating cells. In that latter case, low values of  $\rho_{HV}$  are probably due to reflectivity gradients across the beam (Ryzhkov 2007);

□ A variety of  $Z_{DR}$  values have been found in hail-bearing cells (confirmed by ground observations) : values ranging from very negative (-5 dB,

corresponding probably to hailstones falling with their major axis along the vertical, Zrnic et al. 1993) to very positive (+5 dB, corresponding to giant melting hailstones, Rasmussen and Heymsfield 1987) passing through the classically expected 0 dB. Cases of melting hail (very high  $Z_{DR}$  values and very low  $\rho_{HV}$  values) may be confused with heavy rain with resonance effects.  $K_{DP}$  may be helpful in that situation but it should be kept in mind that  $K_{DP}$  is not directly measured but estimated from a filtered (2 – 6 km)  $\phi_{DP}$  profile. That might lead to differences with expected intrinsic  $K_{DP}$  values (based, say, on T-matrix scattering simulations). Membership functions for hail, melting hail and heavy rain will have to be revisited in the near future using both T-matrix scattering simulations and observations.

□ The extremely high space-time variability of hail patterns make the objective validation of radar diagnostics complicated. Issues such as 1) temporal interpolation between two successive 5' radar hail maps, 2) horizontal drift between the radar beam height and 3) the ground and radar pixel – hailpad geographical matching have to be carefully addressed.

□ The identification of melting hail at the radar beam height does not mean that hail will fall at ground. The Rasmussen and Heymsfield (1987) hailstone melting model should be considered in the future to extrapolate the radar diagnostics down to ground level.

□ The quantification of the hailstone diameter is important because it is directly related to the damages. In our case, hailpads are sensitive to hailstones with diameters larger than 5 mm. Thus, in an objective evaluation of polarimetric hail detection techniques, only radar hail detections of diameters larger than 5 mm should be taken into account.

## References

- Amburn, S.A., and P. L. Wolf, 1997 : VIL density as a Hail indicator, *Wea. Forecasting*, **12**, 473 – 478.
- Donaldson, R. J. J., 1959: Analysis of severe convective storms observed by radar—II. *J. Meteor.*, **16**, 281–287.
- Delobbe, L., and I. Holleman, 2006 : Uncertainties in radar echo top heights used for hail detection, *Meteorol. Appl.*, **13**, 361 – 374.
- Dupuy, P., A. Kergomard, P. Tabary and O. Bousquet, 2009 : Real-time nation-wide production of 3D wind and reflectivity fields in France : science, engineering and applications, 34<sup>th</sup> Radar Conference, 5 – 9 October, Williamsburg, VA, USA.
- Gourley, J. J., P. Tabary, and J. Parent du Chatelet, 2006a : Data quality of the Meteo-France C-band polarimetric radar. *J. Atmos. Oceanic Technol.*, **23**, No. 10, 1340–1356.
- , P. Tabary, and J. Parent du Chatelet, 2006b: Empirical estimation of attenuation from differential propagation phase measurements at C-band. *J. Appl. Meteor.*, **46**, No. 3, 306 – 317.
- Gourley, JJ, P. Tabary, J. Parent-du-Chatelet, 2007: A fuzzy logic algorithm for the separation of precipitating from non-precipitating echoes using polarimetric radar, *J. Atmos. Oceanic Technol.* Vol. **24**, No. 8, 1439–1451.
- Gourley, JJ., A.J. Illingworth and P. Tabary, 2009 : Absolute calibration of radar reflectivity using redundancy of the polarization observations and implied constraints on drop shapes, *Journal of Atmospheric and Oceanic Technology*, Volume **26**, Issue 4 (April 2009) pp. 689–703.
- Marzano F.S., D. Scaranari, M. Celano, P.P. Alberoni, G. Vulpiani, M. Montopoli, 2006: Hydrometeor classification from dual-polarized weather radar: extending fuzzy logic from S-band to C-band data, *Adv. in Geosci.*, **7**, 109-114.
- Marzano F.S., D. Scaranari, and G. Vulpiani, 2007: Supervised fuzzy-logic classification of hydrometeors using C-band dual-polarized radars. *IEEE Trans. Geosci. Rem. Sensing*, **45**, 3784-3799.
- Park, H.S., A. V. Ryzhkov, D. S. Zrnić, and Kyung-Eak Kim, 2009 : The Hydrometeor Classification Algorithm for the Polarimetric WSR-88D: Description and Application to an MCS *Weather and Forecasting* Volume 24, Issue 3 (June 2009) pp. 730–748.
- Rasmussen, R. M., and A. J. Heymsfield, 1987: Melting and Shedding of Graupel and Hail. Part 1: Model Physics. *J. Atmos. Sci.*, **44**, 2754-2763.
- Ryzhkov, A.V., 2007 : The Impact of Beam Broadening on the Quality of Radar Polarimetric Data, *Journal of Atmospheric and Oceanic Technology*, **24**, No 5, 729–744.
- Tabary, P., Vulpiani, G., J.J. Gourley, A.J. Illingworth, R.J. Thompson and O. Bousquet, 2009 : Unusually high differential attenuation at C-band : results from a two-year analysis of the French Trappes polarimetric radar data, to appear in *J. Appl. Meteor.*
- Vinet, F., 2001: Climatology of Hail in France, *Atmos. Res.*, **56**, 309 – 323.
- Vulpiani, G., P. Tabary, J. Parent-du-Chatelet and Frank S. Marzano, 2008 : Comparison of advanced radar polarimetric techniques for operational attenuation correction at C-band, *J. Atmos. Oceanic Technol.*, **25**, Issue 7 (July 2008) pp. 1118–1135.
- Waldvogel, A., B. Federer, and P. Grimm, 1979: Criteria for the detection of hail cells. *J. Appl. Meteor.*, **18**, 1521–1525.
- Zrnić, D. S., V. N. Bringi, N. Balakrishnan, K. Aydin, V. Chandrasekar, and J. Hubbert, 1993: Polarimetric measurements in a severe hailstorm. *Mon. Weather Rev.*, **121**, 2223-2238.